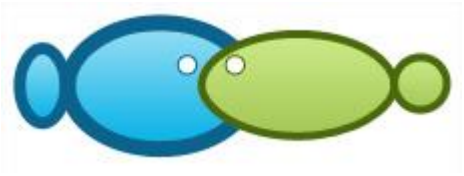

Preparation model and standardization of potentially anti-cancer hydroxyapatite nanoparticles from *Tegillarca granosa* shells

[1,2]Nur Fadhilah, [1,3]Retno P. Rahayu, [1,4]Heny Arwati, [1,5]Nunuk D. R. Lastuti, [1,2]Yan Fuana, [1,3]Theresia I. Budhy

[1] Postgraduate School, Airlangga University, Surabaya, Indonesia; [2] Department of Immunology, Postgraduate School, Airlangga University, Surabaya, Indonesia; [3] Department of Oral Pathology and Maxillofacial, Faculty of Dental Medicine, Airlangga University, Surabaya, Indonesia; [4] Department of Medical Parasitology, Faculty of Medicine, Airlangga University, Surabaya, Indonesia; [5] Department of Veterinary Parasitology, Faculty of Veterinary Medicine, Airlangga University, Surabaya, Indonesia. Corresponding author: R. P. Rahayu, a-retno-p-r@fkg.unair.ac.id

Abstract. Cancer is the second leading cause of death worldwide, which was responsible for approximately 9.6 million fatalities in 2018. Cancer treatment innovations are very diverse: namely chemotherapy, radiotherapy, immunotherapy, surgery and combinations of these therapy techniques. Therefore, the formulation of a new therapy strategy is required to inhibit the growth of cancer cells without major side effects and economical reasons. Hydroxyapatite-based biomaterial has been applied as anti-cancer because it has a good biocompatibility and bioactivity. *Tegillarca granosa* contains a high percentage of $CaCO_3$, which is also the source of calcium for hydroxyapatite synthesis. The general objective of this study is to obtain standardized hydroxyapatite nanoparticles from *T. granosa* shells as potential anti-cancer materials. The hydroxyapatite synthesis employed the hydrothermal method by utilizing High Energy Milling tools to alter the size into nanoparticles. The sample characterization methods used were PSA, FTIR, SEM-EDX, XRD and the cytotoxicity test with MTT assay. The result with XRD spectra showed that the sample had crystallized well. Furthermore, the SEM-EDX analysis had a Ca/P ratio of 1,67. The development of the PSA test was 183.6 nm. Based on the cytotoxicity test, the development of the cell viability showed that the nHAP was not toxic in a typical cell environment. This study concludes that the yield of synthesis of hydroxyapatite nanoparticles from the clam's shell of *T. granosa* had significant results and it was reaching the HAp standard, also having a potential as cancer treatment.

Key Words: hydroxyapatite, nanoparticles, hydrothermal, *Tegillarca granosa* shells, anti-cancer.

Introduction. The common challenge in cancer treatment is the negative effect of the chemo-therapy, which affects also normal cells, and leads to the drug resistance of tumors and large drug circulation spans (Rao 2016). Therefore, a new therapy strategy is required to selectively kill cancer cells without affecting normal cells, one of which is the discovery of compounds that base their targeted action on genes that regulate growth, differentiation and cell death by utilizing materials available in nature.

Tegillarca granosa or commonly called blood clams belong to the bivalves class with the order Arcida. This clam is a species with a very high distribution in Southeast Asia, especially in Indonesia (Mirzaei et al 2014). The abundance of clam blood in Indonesia in 2011, according to the Direktorat Jendral Perikanan Tangkap (2012), was of 39,000 tons. Blood clams are mostly used for food, so the shells will become waste. The use of shells is variable, including handicrafts and animal feed mixtures (Boey et al 2011). Moreover, to avoid damaging impacts on the environment, blood shells can also be transformed into a potential aggregation substitute in concrete and can be used in the medical field, because the clamshell contains many minerals.

The high concentration of $CaCO_3$ can be used as a source of calcium for the synthesis of hydroxyapatite (HAp). The hydroxyapatite-based biomaterial has been

applied as anti-cancer because it has a good biocompatibility and bioactivity (Zhang et al 2019). Shi et al (2009) revealed that HAp could inhibit proliferation and induce apoptosis in cancer cells of osteosarcoma. Moreover, HAp can inhibit gastric cancer cells (Chen et al 2007), cancer cells of the colon (Dey et al 2014) and liver cancer cells (Ezhaveni et al 2013).

Several techniques in processing the synthesis of hydroxyapatite include precipitation, hydrolysis, sol-gel and hydrothermal. The hydrothermal method is the most widely used technique because it is a more efficient and more accessible process (Azis et al 2015). In its application, nano-hydroxyapatite (nHAp) must meet several criteria (Afriani et al 2020). The standard size of the particle to be used as an anti-cancer therapy, tested with particle size analyzer (PSA), is less than 1 μm, with a length of less than 200 nm (Fox et al 2012). A scanning electron microscope (SEM) test is performed for observing the particles morphology and the stoichiometry of the Ca/P ratio. A good Ca/P ratio is 1.67, because if the molar value is less, the nHAp will be more soluble (Dorozhkin et al 2010). Standard nHAp compound structure tested with Fourier-transform infrared spectroscopy (FTIR) is Ca^{2+}, $(PO_4)^{3-}$ and OH^- (Uskoković & Uskoković 2010).The nHAp crystallographic structure tested with x-ray diffraction (XRD) is characterized by the JCPDS no. 9-432 reference standard, which means that the hydroxyapatite nanoparticle crystallizes well and has a regular structure, in the nHAp sample (ISO 13779-1 2008).

Material and Method

Synthesis of T. granosa shell into hydroxyapatite. The synthesis process was started by washing the blood clam shells, then boiling them for 10 minutes and drying them under the sun for 24 hours. The shells were then mashed using a mortar and sieved using 200 and 400 mesh sieves. $CaCO_3$ powder was calcined at 1000°C for 10 hours to form CaO. 20.8 g of CaO powder was soaked with H_2O for 24 hours to form $Ca(OH)_2$. The soaked powder was then dried. 25.1 mL of HNO_3 solution was prepared, which was then dissolved in distilled water until 100 mL. Then, 39.44 g of $(NH_4)_2HPO_4$ was prepared and diammonium hydrogen phosphate (DHP) was dissolved in distilled water up to 100 mL. 36.9 g of $Ca(OH)_2$ powder obtained was mixed into HNO_3 solution, then stirred until getting homogeneous, for 30 minutes, at room temperature, at 700 rpm. After stirring, the $Ca(NO_3)_2{\cdot}2H_2O$ solution was then mixed with the $(NH_4)_2HPO_4$ solution at 700 rpm at 30°C. 13.96 mL of NH_4OH was added so that an alkaline environment (pH 9-10) was obtained, determined with a PP indicator. The precipitate was washed with DI water until the color of the PP indicator disappeared, then filtered using fine filter paper and annealing precipitate at 100°C. HAp powder was then in the furnace at 1000°C, for 2 hours. The equation of compound formed was as follows (Pham Min et al 2014):

$$10Ca(NO_3)_2.4H_2O_{(aq)} + 6(NH_4)_2HPO_{4(aq)} + 8NH_4OH_{(aq)} \rightarrow Ca_{10}(PO_4)_6(OH)_2(s) + 20NH_4NO_3(aq) + 46H_2O(I)$$

Synthesis of hydroxyapatite nanoparticles. The HAp powder produced in the preceding phase was then milled using a milling ball at the mass ratio of 1:20, for a milling period of 9 hours. The HA powder and alumina ball milling were then weighed based on the ratio and placed in the milling vial. The milling was done repeatedly, until reaching the required total time (Aminatun et al 2019).

Characterization of hydroxyapatite nanoparticles from T. granosa shells. the characterization of the sample by the PSA test required a solvent in the form of distilled water. SEM (FEI, Inspect S50) in the Universitas Negeri Malang, Indonesia with 2.000x magnification was used to characterize the particle size and grain shape. FTIR (Shimadzu IR Prestige 21) from the Tenth of November Institute of Technology Indonesia required 2 mg of samples, blended with 100 mg KBr, to make pellets with a vacuum press. The infrared light absorption spectrum of the pellets was in the wave range of 4,000-400 cm^{-1}.

XRD (PanAnalytical Merck Xpert Pro) from the Tenth of November Institute of Technology Indonesia required the degree of crystallinity of 2θ. An MTT Assay containing tetrazolium salt [3(4,5-dimetiltiazol-2-yl)-2,5-difeniltetrazolium bromide] was used to test the cell viability. The MTT Assay method's principle is based on the mitochondrial activities ability of the living cells, demonstrated in the cell culture. The Vero cell was employed in this experiment. The basic technique of MTT Assay was the conversion of tetrazolium salt [3-(4,5-dimetiltiazol-2-yl)-2,5-difeniltetrazolium bromide] to formazan in active mitochondria, determined by an Elisa reader at 560 and 750 nm. The living cell will convert MTT to formazan, via the reduction of reductase enzyme in a chain of the mitochondrial respiratory system.

Data analysis. The results of SEM-EDX research was analyzed using the ImageJ application. The results of the XRD research was analyzed using the Xpert HSP application, followed by the Origin application. The results of the cytotoxicity study was analyzed with Microsoft Excel by calculating the percentage of life which is converted to the CC50 value. This value indicates a concentration that can inhibit 50% of living cells.

Results

PSA test. PSA test was used to find out the diameter of hydroxyapatite nanoparticles. Particle analysis was preceded by dissolving samples into a liquid media, followed by a sonication process. Samples must be dissolved with distilled water first, so that there is no agglomeration on particles to ensure that the measured size corresponds to a single particle. A particle test using PSA for 9 hours obtained a size of 183.6 nm.

SEM-EDX test. Analysis of morphology and distribution of particle sizes was tested using SEM-EDX with 2000 X magnification. Testing with SEM-EDX was conducted to observe the morphology of hydroxyapatite and to analyze the chemical components and the ratio of Ca:P. The results of morphology study with SEM are presented in Figure 1. Results of SEM shown in Figure 1 revealed an inhomogeneous morphology with irregular needle-shaped particles and an inhomogeneous size distribution of the samples. Particles overlap and create a bigger group. Besides finding out the morphology, SEM can determine the particle size distribution of HAp. The particle size distribution was analyzed using the ImageJ application. The results of particle size distribution data were 50.47 nm-881.52 nm. The results of the EDX test can be seen in Table 1. The results of the Ca:P ratio analysis were seen from the atomic percentage (At) value obtained from EDX.

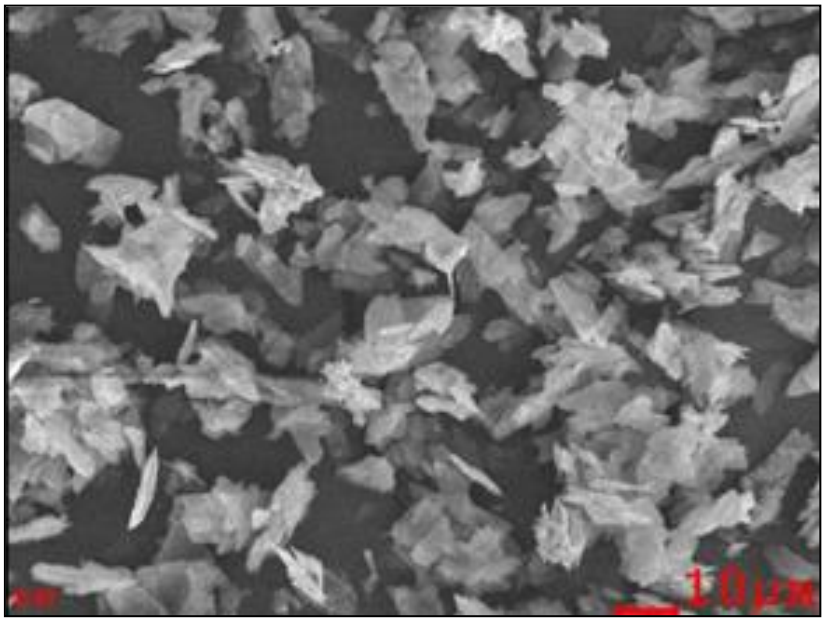

Figure 1. The results of particle morphology with 2000 X magnification.

Table 1

Composition of element and ratio of Ca/P

Element	*Wt %*	*At %*
OK (Oxygen)	41.75	64.04
PK (Phosphorus)	18.57	13.47
CaK (Calcium)	39.68	22.49
Matrix	Correction	ZAF

FTIR test. FTIR test was used to find out the molecular structure formed in the hydroxyapatite samples from *T. granosa* shells. The results of FTIR test for hydroxyapatite had a phosphate (PO_4^{3-}) absorption band with peaks for the wavenumbers of 1,054, 983, 869, 653, 574 and 519 cm^{-1}. The hydroxil (OH^-) absorption peaks had the wavenumbers of 3,472 and 3,165 cm^{-1}. The functional group of Ca-0 phase compounds in this structure was found at the wavenumber of 1,644 cm^{-1}.

XRD test. The test results of XRD using Xpert HSP showed the results of the percentage of the compound in the samples. Then, they were processed against the results of the graph with origin lab to find out the results of intensity and degree of crystallinity. The degree of crystallinity obtained was 85.13%. The highest intensity peak in the samples was in the range of 30°-35°. The highest intensity peak in 2θ=31,82994°. The results were then compared to the data of the JCPDS 9-432 reference standard (Azzaoui et al, 2013) to determine the diffraction peak produced. The index of crystallinity for the results of the XRD test analysis was 85.31459%.

Cytotoxicity test. The cytotoxicity of HAp nanoparticles from *T. granosa* shells was tested using the MTT method in normal cells (Vero cell line). The cytotoxicity test on normal cells aims to find out the toxic effect of samples by looking at the percentage of living cells. The viability of normal cells increased at lower concentrations, which can be seen in Figure 2. The concentrations of toxicity test on Vero cells were 500, 250 and 125 µg mL^{-1}, and the percentage of cell viability result were 88.74%, 94.23% and 103.01%, respectively with a CC50 value exceeding 500 µg mL^{-1}.

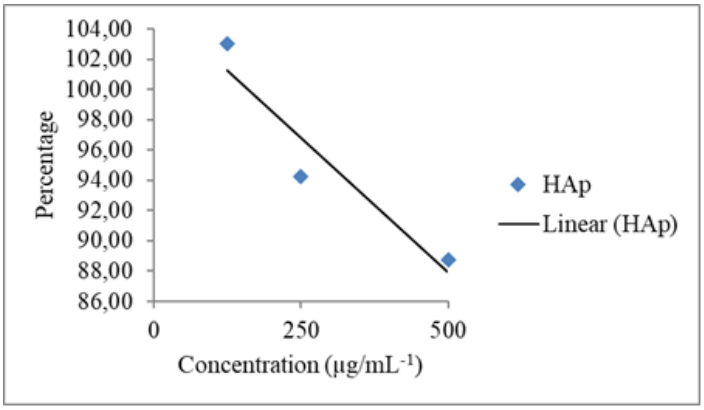

Figure 2. The percentage of cell viability.

Discussion

PSA test. The PSA test result of 183.6 nm can be categorized as nanoparticles. Prabha et al (2016) defined nanoparticles as particles with a size in the range of 1 to 1,000 nm. This is also supported by Hamidi et al (2008), stating that nanoparticles generally vary from 10 to 1,000 nm. Moreover, the study results showed similarity with Aminatun et al (2019), regarding the size of hydroxyapatite particles from the fishbone of *Sepia* sp. that has a size range of 65.26 to 200.20 nm, determined with a High Energy Milling method performed for 9 hours. Based on Dey et al (2014), nHAp's particle size of 1,774 can

inhibit the proliferation of the colon cancer cells HCT116. Sathiyamoorthi et al (2013) also reported that a size of nHAp of less than 1,000 nm can be used as a treatment for liver cancer because the viability of cancer cells is reduced by 30-50%.

SEM-EDX test. Dorozhkin (2010) explained that the standard ratio of Ca/P is 1.67. The ratio of 1.67 means that the ratio of calcium molar and phosphorus are 1-2:1 (Loughrill et al 2016). This is explained by Koutsopoulos (2002), which stated that pure stoichiometric HAp has a composition of 39.68 wt% Ca, 18.45 wt% P, with a Ca/P weight ratio of 2.15 and Ca/P atomic ratio of 1.67. The hydroxyapatite is ipure and it has a good thermal stability, with a ratio proportion that is suitable with the body fluids (Suchanek et al 2004).

FTIR test. Mondal et al (2017) reported that the FTIR spectrum testhas the wavelengths of 479, 567, 605, 1046 and 1098 cm^{-1} for the characteristic band for PO_4^{3-}, and of 3,450–3,575 cm^{-1} and 634 cm^{-1} for the absorption band of OH^- ion, that is able to increase ROS in bone cancer, causing the mitochondrial pathway of cells apoptosis.

XRD test. According to the study by Dey et al (2014), the pattern of XRD test results with diffraction peak of 2θ is 26°, 32°, 40°, 47° and 50°, which is in accordance with the standard of hydroxyapatite XRD pattern (JCPDS09-0432), that is able to inhibit proliferation in HCT116 colon cancer cells. The results of the study by Sathiyamoorthi et al (2013) also reported that nHAp adjusted to the standard of JCPDS 09-0432 is able to stop proliferation in liver cancer cells.

Cytotoxity test. The results of the analysis showed that nHAp from *T. granosa* shells were not toxic to Vero cells. This remark is consistent with Abid et al (2012), explaining that the cytotoxic concentration of 50% (CC50) is defined as the compound concentration (g mL^{-1}) necessary for a 50% loss in cell viability, as computed by regression analysis. This is supported by Ariani et al (2009), who explained that a particle is considered aș not toxic if it has a percentage of cell viability of more than 50%.

Nanoparticle hydroxyapatite effect to cancer cell. The application of standardized hydroxyapatite nanoparticles has a potential as an anti-cancer therapy because hydroxyapatite nanoparticles can trigger apoptosis and inhibit cancer cell proliferation (Zhang et al 2019). The nHAp is able to reach cancer cells through intravenous injection; when taken orally, it cannot penetrate (Khalifehzadeh & Arami 2020). Because saliva includes minerals, proteins such as immunoglobulins, enzymes, mucins and nitrogen compounds, hydroxyapatite nanoparticles cannot permeate the oral mucosa. (Humphrey & Williamson 2001). Saliva has defensive properties against solid particles, due to the corona proteins. The protein is known to cause nanoparticle aggregation, to increase their size and to change their surface function, reducing the number of nanoparticles uptaken into the cell and destroying the trapped particles within minutes. (Min et al 2015). It implies that some of the nHAP present in the oral cavity are possibly trapped by mucus and do not seep into the epithelial cell layers (Aljayyoussi et al 2012).

Appropriate dosage of intravenous injections with nHAp can produce an excellent targeting effect on the cancer cells and is safe. The nHAp with an optimum particle length of around 50-200 nm is promptly ingested and removed by reticuloendothelial system macrophages (histiocytes), most of which will migrate to the lymph nodes via the vessels-spleen (Arami et al 2015). Appropriate size nHAp nanoparticles can directly penetrate lymph nodes (Porter & Trevaskis 2020). The lymph nodes will filter the lymph out through the efferent lymphatic vessels and drive the nanoparticles out into the veins (Du et al 2021). Because of the high density of lymphatic capillaries in the dermis, intradermal administration of drug delivery systems has demonstrated a high lymphatic absorption (Permana et al 2021). Lymphatic capillaries will absorb formulations with particles ranging in size from 50 to 200 nm (Porter & Trevaskis 2020). The bigger particles will settle on the skin, while the smaller particles will be absorbed by the blood capillaries (Permana et al 2021). Finally, nHAp can be distributed to cancer areas through

the lymphatic system because of its ionic charge (Du et al 2021). Hydroxyapatite consists of 2 types of ions on its surface, namely Ca^{2+} and PO_4^{3-}. The presence of positive ions in hydroxyapatite can serve to determine the negative charge around cancer cells. Cancer cells have more negative charge than normal cells due to an abundance of negatively charged groups on their surface, which is obtained from sialic acid residues projecting from the apical surface of the plasma membrane. nHAP is expected to have more adhering capacity to cancer cells than to normal cells, due to electrostatic interactions between negatively charged sites on the cell membrane and positive binding sites on the HAp surface (Han et al 2014).

Cancer cells have a higher endocytosis activity than normal ones (Qiang et al 2008). The presence of chemical compounds like PO_4^{3-} on nHAp, that enter the cytoplasm of cancer cells, can cause cells to experience intracellular oxidative stress and increase ROS (Xu et al 2011). Increased ROS will cause protein caspase activation and cause cancer cell apoptosis in the mitochondrial pathway (Yuan et al 2010). Hydroxyapatite nanoparticles can activate mitochondrial pathway apoptosis because a chemical (hydroxyapatite) disrupts mitochondria and activates the p53 protein (Xu et al 2011). The activation of p53 protein will cause the release of cytochrome C from the mitochondrial intermembrane. Then Bcl-2 is activated by BH3-protein that forms Bax. Cytochrome C binds to APAF-1 to form the apoptosome and activates procaspase 9 and then activates caspase-9. Furthermore, caspase 9 will activate procaspase-3, cellular and nucleosome fragmentation (Anita et al 2014).

In addition to apoptosis, Wang et al (2017) reported that HAp composites could recruit macrophages to produce TNF-α. As death receptors, the TNF superfamily can directly trigger cell apoptosis via an extrinsic pathway with pro-inflammatory cytokines (Pasparakis & Vandenabeele 2015). Ward-Kavanagh et al. (2016) also explained that TNF cytokines, found in tumor in vivo samples treated with nHAp, can inhibit tumorigenesis. The research results by Guo et al (2019) explained that the expression of NF-κB in glioma cells with HAp treatment decreased. Activation of NF-κB signaling can suppress apoptosis, leading to cancer development, so that if NF-κB expression is inhibited, cells can undergo apoptosis (Van et al 1996). Wang et al (2016) reported that HAp could activate IFN-γ in vitro. The presence of IFN-γ expression indicates NK cell activity (Schoenborn & Wilson 2007). IFN-γ can stimulate NK cells directly, thereby increasing their cytotoxicity (Dewanti et al 2012). NK cells have a role in destroying cancer cells (Kurahara et al 2009). If there is an increase in IFN-γ, then NK cells will be active and they can kill cancer cells, through the bond between FasLigand (CD95R) on the surface of cancer with Ligand (CD95) on the surface of NK cells. With this bond, NK cells will release perforin and granzyme B molecules, causing apoptosis in cancer cells (Mitra et al 2003).

Conclusions. The results of the synthesis of hydroxyapatite from *T. granosa* shells were particles of a size of 183.6 nm, determined with a PSA test. The results for the particle size distribution with a SEM test indicated a range of 50.47-881.52 nm. Ca/P ratio in the samples was obtained by SEM-EDX, with a result of 1.67, corresponding to the pure Hydroxyapatite. The structure of the compound in HAp nanoparticles was analyzed with FTIR. Ca^{2+}, OH^- and PO_4^{3-} were commonly found in the typical structure of nHAp. The XRD results were in accordance with the JCPDS standard (09-0432), indicating that nHAp has a high degree of crystallinity, of 85.31459%, suggesting regularity in the structure of nHAp samples. The cytotoxicity test revealed that samples were not toxic, with a normal cell viability >90%. The *T. granosa* shell can be synthesized into standardized nHAp which has an anti-cancer potential.

Conflict of interest. The authors declare no conflict of interest.

References

Abid N. B., Lassoud M. A., Aouni M., 2012 Assessment of the cytotoxic effect and in vitro evaluation of the anti-enteroviral activities of plants rich in flavonoids. Journal of Applied Pharmaceutical Care 2(5):74-78.

Afriani F., Siswoyo, Amelia, Ririn, Hudatwi M., Zaitun, Tiandho, Yuant, 2020 Hydroxyapatite from natural sources: methods and its characteristics. IOP Conference Series: Earth and Environmental Science 599:1-7.
Aljayyoussi G., Abdulkarim M., Griffiths P., Gumbleton M., 2012 Pharmaceutical nanoparticles and the mucin biopolymer barrier. Bioimpacts 2:173–174.
Aminatun, Supardi A., Nisa Z. I., Hikmawati D., Siswanto, 2019 Synthesis of nanohydroxyapatite from cuttlefish bone (*Sepia* sp.) using milling method. Hindawi International Journal of Biomaterials, pp. 1-6.
Anita, Sharma H. P., Paras J., Patnaik A., 2014 Apoptosis (programmed cell death) – a review. World Journal of Pharmaceutical Research 3(4):1854-1872.
Ariani M. D., Yuliati A., Adiarto T., 2009 Toxicity testing of chitosan from tiger prawn shell waste on cell culture. Dental Journal 42(1):15–20.
Arami H., Khandhar A., Liggitt D., Krishnan K. M., 2015 In vivo delivery, pharmacokinetics, biodistribution and toxicity of iron oxide nanoparticles. Chemical Society Reviews 44(23):576–607.
Azis Y., Novesar J., Syukri A., Hadi N., 2015 Facile synthesis of hydroxyapatite particles from cockle shells (*Anadara granosa*) by hydrothermal method. Orientjchem 31(2):1-8.
Boey P. L., Maniam G. P., Hamid S. A., Ali D. M. H., 2011 Utilization of waste cockle shell (*Anadara granosa*) in biodiesel production from palm olein: Optimization using response surface methodology. Fuel 9(1):2353–2358.
Chen X., Deng C., Tang S., Zhang M., 2007 Mitochondria-dependent apoptosis induced by nanoscale hydroxyapatite in human gastric cancer sgc-7901 cells. Biological & Pharmaceutical Bulletin 30(1):128–132.
Dey S., Das M., Balla V. K., 2014 Effect of hydroxyapatite particle size, morphology and crystallinity on proliferation of colon cancer HCT116 cells. Materials Science and Engineering:C 3(9):336–339.
Dorozhkin S. V., 2010 Bioceramics of calcium orthophosphates. Biomaterials 31(7): 1465–1485.
Du M., Chen J., Liu K., Xing H., Song C., 2021 Recent advances in biomedical engineering of nano-hydroxyapatite including dentistry, cancer treatment and bone repair. Composites Part B: Engineering 215:1-23.
Ezhaveni S., Yuvakkumar R., Rajkumar M., Sundaram N. M., Rajendran V., 2013 Preparation and characterization of nano-hydroxyapatite nanomaterials for liver cancer cell treatment. Journal of Nanoscience and Nanotechnology 13(3):1631–1638.
Fox K., Tran P. A., Tran N., 2012 Recent advances in research applications of nanophase hydroxyapatite. ChemPhysChem 13(10):2495–2506.
Guo G., Tian A., Lan X., Fu C., Yan Z., Wang C., 2019 Nano hydroxyapatite induces glioma cell apoptosis by suppressing NF κB signaling pathway. Experimental and Therapeutic Medicine 17(2019):4080-4088.
Hamidi M., Azadi A., Rafiei P., 2008 Hydrogel nanoparticles in drug delivery. Advanced Drug Delivery Reviews 60(15):1638–1649.
Han Y., Li S., Cao X., Yuan L., Wang Y., Yin Y., Tong Q., Honglian D., Wang X., 2014 Different inhibitory effect and mechanism of hydroxyapatite nanoparticles on normal cells and cancer cells in vitro and in vivo. Scientific Reports 4(1):1-7.
Humphrey S. P., Williamson R. T., 2001 A review of saliva: Normal composition, flow, and function. Journal of Prosthetic Dentistry 85(2001):162–169.
Khalifehzadeh R., Arami H., 2020 Biodegradable calcium phosphate nanoparticles for cancer therapy. Advances in Colloid and Interface Science 279:1-20.
Koutsopoulos S., 2002 Synthesis and characterization of hydroxyapatite crystals: A review study on the analytical methods. Journal of Biomedical Materials Research 62(4):600–612.
Kurahara H., Hiroyuki S., Yuko M., Kousei M., Hidetosteosarkomahi N., Fumitake K., Masahiko S., Shinichi U., Shoji N., Sonshin T., 2009 Significance of M2 polarized tumor-associated macrophage in pancreatic cancer. Journal Surgical Research 167(2):e211-e219.

Loughrill E., Wray D., Christides T., Zand N., 2016 Calcium to phosphorus ratio, essential elements and vitamin D content of infant foods in the UK: Possible implications for bone health. Maternal & Child Nutrition 13(3):1-10.
Min L., Jian Z., Wei S., Yuan H., 2015 Developments of mucus penetrating nanoparticles. Asian Journal of Pharmaceutical Sciences 10:275–282.
Mirzaei M. R., Yasin Z., Hwai A. T. S., 2014 Length-weight relationship, growth and mortality of Anadara granosa in Penang Island, Malaysia: an approach using length-frequency data sets. Journal of the Marine Biological Association UK 95(2):381–390.
Mitra R., Singh S., Khar A., 2003 Antitumour immune responses. Expert Reviews in Molecular Medicine 5(3):1-19.
Mondal S., Manivasagan P., Bharathiraja S., Santha Moorthy M., Nguyen V. T., Kim H. H., Nam S. Y., Lee K. D., Oh J., 2017 Hydroxyapatite coated iron oxide nanoparticles: a promising nanomaterial for magnetic hyperthermia cancer treatment. Nanomaterials 7(12):426.
Pasparakis M., Vandenabeele P., 2015 Necroptosis and its role in inflammation. Nature 517(7534):311–320.
Permana A. D., Nainu F., Moffatt K., Larrañeta E., Donnelly R. F., 2021 Recent advances in combination of microneedles and nanomedicines for lymphatic targeted drug delivery. WIREs Nanomedicine and Nanobiotechnology 13(3):1-22.
Pham Minh D., Rio S., Sharrock P., Sebei H., Lyczko N., Tran N. D., Nzihou A., 2014 Hydroxyapatite starting from calcium carbonate and orthophosphoric acid: synthesis, characterization, and applications. Journal of Materials Science 49(12):4261–4269.
Porter C. J. H., Trevaskis N. L., 2020 Targeting immune cells within lymph nodes. Nature Nanotechnology 15:423-425.
Prabha S., Geeta A., Ramesh C., Bahar A., Surendra N., 2016 Effect of size on biological properties of nanoparticles employed in gene delivery. Artificial Cells Nanomedicine and Biotechnology 44(1):83-91.
Qiang F., Rahaman M. N., Nai Z., Wenhai H., Deping W., Liying Z., Haifeng L., 2008 In vitro study on different cell response to spherical hydroxyapatite nanoparticles. Journal of Biomaterials Applications 23(1):37–50.
Rao P. V., Nallappan D., Madhavi K., Rahman S., Jun Wei L., Gan S. H., 2016 Phytochemicals and biogenic metallic nanoparticles as anticancer agents. Oxidative medicine and cellular longevity. Hindawi Publishing 20(16):1–15.
Sathiyamoorthi E., Rathinam Y., Mani R., Nachiappan M. Venkatachalam R., 2013 Preparation and characterization of nano-hydroxyapatite nanomaterials for liver cancer cell treatment. Journal of Nanoscience and Nanotechnology 12:1-8.
Schoenborn J. R., Wilson C. B., 2007 Regulation of interferon-gamma during innate and adaptive immune responses. Advances in Immunology 96:41-101.
Shi Z., Huang X., Cai Y., Tang R., Yang D., 2009 Size effect of hydroxyapatite nanoparticles on proliferation and apoptosis of osteoblast-like cells. Acta Biomaterialia 5(1):338–345.
Suchanek W. L., Byrappa K., Shuk P., Riman R. E., Janas V. F., TenHuisen K. S., 2004 Preparation of magnesium-substituted hydroxyapatite powders by the mechanochemical–hydrothermal method. Biomaterials 25(19):4647–4657.
Uskoković V., Uskoković D. P., 2010 Nanosized hydroxyapatite and other calcium phosphates: chemistry of formation and application as drug and gene delivery agents. Journal of Biomedical Materials Research Part B: Applied Biomaterials 96B(1):152–191.
Xu Z., Liu C., Wei J., Sun J., 2012 Effects of four types of hydroxyapatite nanoparticles with different nanocrystal morphologies and sizes on apoptosis in rat osteoblasts. Journal of Applied Toxicology 3(2):429–435.
Van A. D. J., Martin S. J., Kafri T., Green D. R. Verma I. M., 1996 Suppression of TNF-alpha-induced apoptosis by NF-kappaB. Science 274(1996):787-789.
Wang X., Li X., Ito A., Watanabe Y., Sogo Y., Hirose M., Tsuji N. M., 2016 Rod-shaped and substituted hydroxyapatite nanoparticles stimulating type 1 and 2 cytokine secretion. Colloids and Surfaces B: Biointerfaces 139:10–16.

Wang J., Liu D., Guo B., Yang X., Chen X., Zhu X., Zhang X., 2017 Role of biphasic calcium phosphate ceramic-mediated secretion of signaling molecules by macrophages in migration and osteoblastic differentiation of MSCs. Acta Biomaterialia 51:447–460.
Ward-Kavanagh L. K., Lin W. W., Šedý J. R., Ware C. F., 2016 The TNF receptor superfamily in co-stimulating and co-inhibitory responses. Immunity 44(5):1005–1019.
Yuan Y., Liu C., Qian J., Wang J., Zhang Y., 2010 Size-mediated cytotoxicity and apoptosis of hydroxyapatite nanoparticles in human hepatoma HepG2 cells. Biomaterials 31(4):730–740.
Zhang K., Zhou Y., Xiao C., Zhao W., Wu H., Tang J., Zhongtao L., Sen Y., Xiangfeng L., Li M., Zhentao Y., Gang W., Lin W., Kai Z., Xiao Y., Xiangdong Z., Chongqi T., Zhang X., 2019 Application of hydroxyapatite nanoparticles in tumor-associated bone segmental defect. Science Advances 5(8):1-16.
*** Direktorat Jendral Perikanan Tangkap, 2012 Statistik perikanan tangkap Indonesia, 2011. Kementrian Kelautan Perikanan, Jakarta, ISSN: 1858-0505 12(1):1-6.
*** ISO 13779-1:2008, 2008 Implants for surgery - Hydroxyapatite - Part 1: Ceramic hydroxyapatite, https://www.iso.org/obp/ui/#iso:std:iso:13779:-1:ed-2:v1:en.

Received: 27 January 2022. Accepted: 22 June 2022. Published online: 09 July 2022.
Authors:
Nur Fadhilah, Department of Immunology, Postgraduate School, Airlangga University, Surabaya, Indonesia, e-mail: nfadhilah10@yahoo
Retno Pudji Rahayu, Department of Oral Pathology and Maxillofacial, Faculty of Dental Medicine, Airlangga University, Surabaya, Indonesia, e-mail: a-retno-p-r@fkg.unair.ac.id
Heny Arwati, Department of Medical Parasitology, Faculty of Medicine, Airlangga University, Surabaya, Indonesia, e-mail: arwatiheny@yahoo.com
Nunuk Dyah Retno Lastuti, Department of Veterinary Parasitology, Faculty of Veterinary Medicine, Airlangga University, Surabaya, Indonesia, e-mail: nunuk_dyah@fkh.unair.ac.id
Yan Fuana, Department of Immunology, Postgraduate School, Airlangga University, Surabaya, Indonesia, e-mail: yanfuana90@gmail.com
Theresia Indah Budhy, Department of Oral Pathology and Maxillofacial, Faculty of Dental Medicine, Airlangga University, Surabaya, Indonesia, e-mail: terebudy@gmail.com

How to cite this article:
Fadhilah N., Rahayu R. P., Arwati H., Lastuti N. D. R., Fuana Y., Budhy T. I., 2022 Preparation model and standardization of potentially anti-cancer hydroxyapatite nanoparticles from *Tegillarca granosa* shells. AACL Bioflux 15(4):1639-1647.